

Lattice Boltzmann method for viscoelastic fluids

Iaroslav Ispolatov^{1,2} and Martin Grant¹

¹*Department of Physics, McGill University, 3600 rue University, Montréal, Québec, Canada, H3A 2T8*

²*Center for Studies in physics and Biology, Rockefeller University, 1230 York Ave, New York, NY 10021, USA.*

(November 13, 2018)

Lattice Boltzmann model for viscoelastic flow simulation is proposed; elastic effects are taken into account in the framework of Maxwell model. The following three examples are studied using the proposed approach: a transverse velocity autocorrelation function for free evolving system with random initial velocities, a boundary-driven propagating shear waves, and a resonant enhancement of oscillations in a periodically driven fluid in a capillary. The measured shear wave dispersion relation is found to be in a good agreement with the theoretical one derived for the Navier-Stokes equation with the Maxwell viscoelastic term.

I. MODEL

Although only slightly more than a decade old, the Lattice Boltzmann (LB) method [1–4] has already gained the status of a versatile simulation tool for homogeneous and heterogeneous flows in various, often very complex, geometries. Inclusion of viscoelastic effects, common for many naturally-occurring fluids, will make the range of application of the LB method even wider. A modification of the standard BGK model [3], suggested in [5], allows for shear wave propagation, which is one of the intrinsic features of viscoelastic fluids. However, the physical foundations of the approach, proposed in [5], are somewhat unclear, since it does not include any memory about an accumulated shear strain. We propose a more general approach, based on a physically transparent Maxwell model of viscoelasticity [6], which exhibits viscoelastic properties and accounts for accumulated stress via exponentially decaying memory function.

Let us for simplicity consider a standard 6-velocity BGK model on a 2D hexagonal lattice, though generalizations for more sophisticated lattice Boltzmann schemes is straightforward. Evolution equations for an i th channel occupation number f_i have the following form [3]:

$$f_i(\vec{r} + \vec{c}_i, t + 1) = f_i(\vec{r}, t) + \lambda \{ f_i(\vec{r}, t) - f_i^{eq}(\vec{r}, t) \}, \quad (1)$$

where equilibrium occupation numbers f_i^{eq} are:

$$f_i^{eq} = \frac{\rho}{6} [1 + 2(\vec{C}_i \cdot \vec{U}) + G \{ (\vec{C}_i \cdot \vec{U})^2 - \frac{U^2}{2} \}]. \quad (2)$$

Here

$$\rho \equiv \sum_{i=1}^6 f_i, \quad \vec{U} \equiv \sum_{i=1}^6 f_i \vec{C}_i \quad (3)$$

are the equilibrium density and velocity at each lattice site, and \vec{C}_i , $i = 1 \dots 6$ are the lattice unit vectors. Performing Chapman-Enskog expansion, one can prove [3,4] that for $G = 4$ these equations reproduce the Navier-Stokes equation with correct convective term.

Maxwell model for viscoelastic media [6] links the elastic part of the stress tensor Π_{ij}^{el} to the rate of strain $D_{ij} = \partial v_i / \partial x_j + \partial v_j / \partial x_i$ via the linear equation with exponentially decaying elastic “memory”:

$$\frac{d\Pi_{ij}^{el}}{dt} = -\frac{\Pi_{ij}^{el}}{\tau} + \frac{\mu}{\tau} D_{ij}, \quad (4)$$

where μ is an elastic coefficient and τ is a memory time. As the 6-velocity BGK model adequately reproduces the Navier-Stokes equation only for incompressible fluids ($\vec{\nabla} \cdot \vec{v} = 0$), in the following we limit our consideration to this case only. Then the viscoelasticity of the fluid can be taken into account by adding the Maxwell elastic stress (body force) term $\vec{F}_{el}(\vec{r}, t)$,

$$\vec{F}_{el}(\vec{r}, t) = \mu \int_{-\infty}^t \exp[-(t-t')/\tau] \Delta \vec{V}(\vec{r}, t') dt' / \tau, \quad (5)$$

to the right-hand side of Navier-Stokes equation. In terms of Chapman-Enskog expansion [3,4] this elastic term has the same order (ϵ^2) as the standard viscous term. Hence to reproduce the elastic term (5) in corresponding continuous (Navier-Stokes) equation we must add its lattice equivalent to the relaxation term in the Lattice-Boltzmann equations (1):

$$f_i(\vec{r} + \vec{c}_i, t + 1) = f_i(\vec{r}, t) + \lambda \{ f_i(\vec{r}, t) - f_i^{eq}(\vec{r}, t) \} + \frac{1}{3} (\vec{F}_{el}(\vec{r}, t) \cdot \vec{C}_i). \quad (6)$$

Here \vec{F}_{el} is calculated similarly to (5), but with the discretized time:

$$\vec{F}_{el}(\vec{r}, t + 1) = \vec{F}_{el}(\vec{r}, t) [1 - \frac{1}{\tau}] + \Delta \vec{U}(\vec{r}, t) \frac{\mu}{\tau}, \quad (7)$$

where Δ is the discrete Laplace operator for the hexagonal lattice:

$$\Delta \vec{U}(\vec{r}, t) = \frac{2}{3} \sum_{i=1}^6 [\vec{U}(\vec{r} + \vec{C}_i, t) - \vec{U}(\vec{r}, t)], \quad (8)$$

and $\vec{U}(\vec{r}_j)$ are equilibrium velocities at sites \vec{r}_j .

The Eqs. (6-8) formally define our model. Thus, to include the Maxwell viscoelastic effects into the standard

LB method, one just needs to add a new local vector field (7) to the standard BKG LB relaxation term (6), which is updated each time step for every lattice site \vec{r} . In the following section we first qualitatively and then quantitatively check the proposed LB method (6) using three examples: a transverse velocity autocorrelation function for free evolving system with random initial velocities, a boundary-driven propagating shear waves, and a resonant enhancement of oscillations in a periodically driven fluid in a capillary.

II. SIMULATIONS AND DISPERSION RELATIONS

To check whether our model have viscoelastic properties at all, we measure the Fourier transform of transverse velocity autocorrelation function $|\tilde{U}_y(k_x, \omega)|^2$, where

$$\tilde{U}_y(k_x, \omega) \equiv \frac{1}{L^2 T} \sum_{x=-L/2}^{L/2} \sum_{y=1}^L \sum_{t=1}^T U_y(x, y, t) e^{-ik_x x} e^{i\omega t}, \quad (9)$$

where

$$k_x = 2\pi n/L, \quad n = -L/2, \dots, L/2, \quad \omega = 2\pi m/T, \quad m = 1, \dots, T. \quad (10)$$

Here the sum on y corresponds to the averaging of $\tilde{U}_y(k_x, \omega)$ on the y coordinate of the sample.

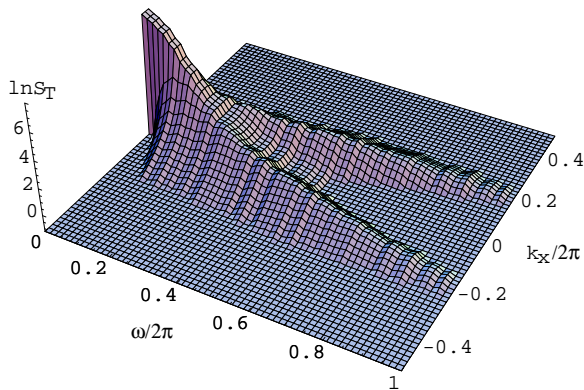


Fig. 1. Sketch of the Fourier transform of the transverse velocity autocorrelation function, $|\tilde{U}_y(k_x, \omega)|^2$, for the LB system with elastic interaction. The axes are $x = \omega/2\pi$, $y = k_x/2\pi$, $z \propto \ln |\tilde{U}_y(k_x, \omega)|$

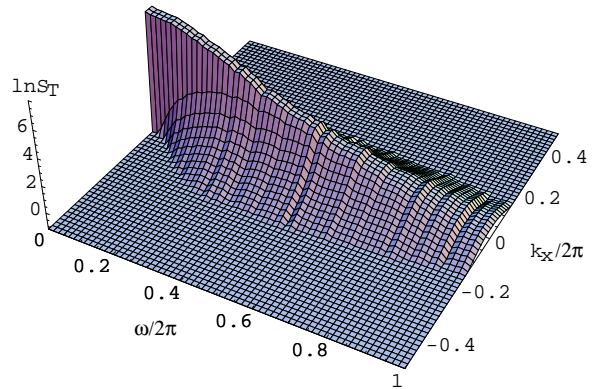


Fig. 2. Sketch of the Fourier transform of the transverse velocity autocorrelation function, $|\tilde{U}_y(k_x, \omega)|^2$, for the LB system without elastic interaction. The axes are $x = \omega/2\pi$, $y = k_x/2\pi$, $z = \propto \ln |\tilde{U}_y(k_x, \omega)|$

In our simulation we use the following parameters: relaxation parameter $\lambda = -1.5$ (which corresponds to viscosity $\nu = 1/4(-1/\lambda - 1/2) \approx 0.042$), elastic coefficient $\mu = 0.3$, memory time $\tau = 10$, lattice of 256×256 sites, maximum time $T = 256$ and random initial occupation numbers corresponding to average density per site $\rho = 1$. The simulation results, averaged over 100 initial configurations, are presented in Fig. 1 and Fig. 2 for the LB models with and without elastic effects, respectively. Two symmetric branches $\omega = \omega(|k_x|)$, clearly noticeable in Fig. 1, which correspond to propagating shear waves, indicate that the LB model defined by (6) indeed exhibits viscoelastic properties.

To get more quantitative insight on the elastic feature of our model, we first derive dispersion relations for the continuous shear waves in the framework of the Maxwell model. Linearized Navier-Stokes equation with Maxwell elastic term for transverse velocity of incompressible fluid reads:

$$\frac{\partial V}{\partial t} = \nu \Delta V + \mu \int_{-\infty}^t \exp[-(t-t')/\tau] \Delta V(t') \frac{dt'}{\tau}. \quad (11)$$

After inserting $V(x, t) = V_0 \exp(-i\omega t) \exp(ikx)$ and discarding exponentially decaying terms, we obtain

$$k^2 = \omega \frac{i + \omega\tau}{\nu(1 - i\omega\tau) + \mu}; \quad (12)$$

or separating real and imaginary parts of k , $\Re(k)$ and $\Im(k)$:

$$k = \sqrt{\frac{\omega}{2[(\mu + \nu)^2 + (\nu\omega\tau)^2]}} \times \left\{ \sqrt{\mu\omega\tau + \sqrt{(\mu\omega\tau)^2 + [\nu(1 + \omega^2\tau^2) + \mu]^2}} + i \sqrt{-\mu\omega\tau + \sqrt{(\mu\omega\tau)^2 + [\nu(1 + \omega^2\tau^2) + \mu]^2}} \right\} \quad (13)$$

We are interested in propagating shear waves with sufficiently small dissipation, hence we consider parameters for which the ratio

$$\frac{\Im(k)}{\Re(k)} = \frac{\nu[1 + (\omega\tau)^2] + \mu}{\mu\omega\tau + \sqrt{(\mu\omega\tau)^2 + [\nu(1 + \omega^2\tau^2) + \mu]^2}} \quad (14)$$

is small. Naively, one can set $\nu\omega^2\tau^2 \ll \mu$ and $\omega\tau \rightarrow +\infty$, thus setting $\Im(k)/\Re(k) \rightarrow (2\omega\tau)^{-1} \rightarrow 0$. But LB systems with too small viscosity and too large elastic coefficient turn out to be numerically unstable. Either for random initial conditions or for small drive, we experimentally determined that domain of stability is roughly limited by $\nu \geq 0.04$ and $\mu \leq 0.3$. For these boundary values of viscosity and elastic coefficient we find that $\Im(k)/\Re(k)$ reaches its minimum when $\omega\tau = \phi \approx 2.9$, at which

$$\Re(k) \approx 0.69, \quad \Im(k) \approx 0.24. \quad (15)$$

To check whether our model reproduces this continuous prediction, we perform the following simulation. We consider a 100×100 lattice with periodic boundary conditions in X direction and reflecting boundary conditions in Y direction. The reflection from the $y = 0$ wall is periodically modulated so that the X components of the velocities after reflection were set to be proportional to $\cos(\omega t)$. Simulations were performed for $\lambda = -1.5$, (or $\nu = 1/4[-1/\lambda - 1/2] \approx 0.042$), elastic coefficient $\mu = 0.3$, memory time $\tau = 46$, and the period of oscillation T corresponded to the theoretical minimum of $\Im(k)/\Re(k)$, $T \equiv 2\pi\tau/\phi \approx 100$.

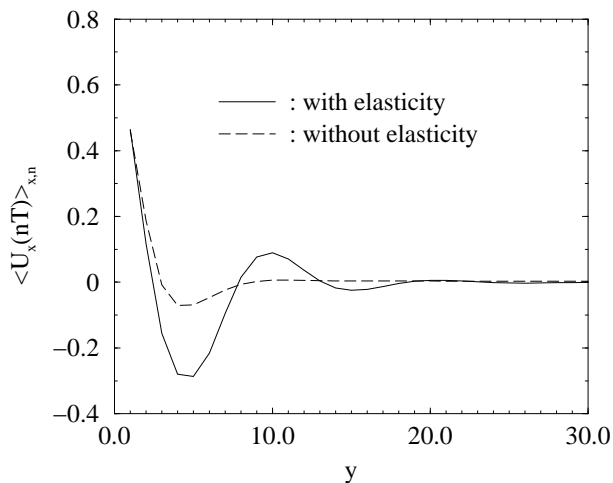


Fig. 3. Plot of the X component of the average velocity $\langle V_x(y, t_n) \rangle_{x,n}$ measured at the times $t_n = nT$, $n = 1, \dots$ vs. the distance from the driving wall y .

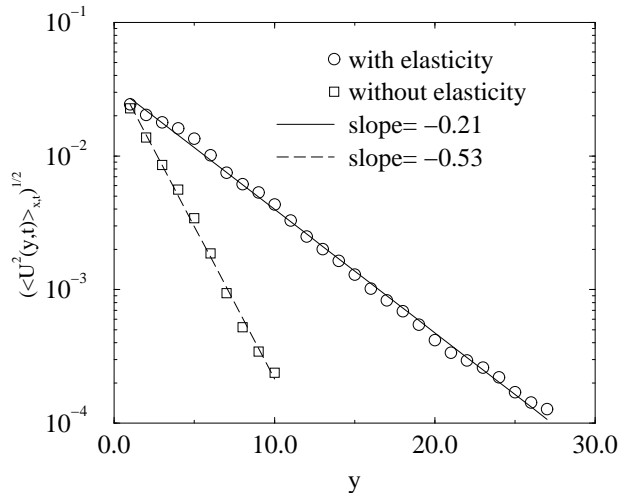


Fig. 4. Square root of the mean square velocity $\sqrt{\langle V_x^2(y, t) \rangle_{x,t}}$ as a function of distance from the driving wall y .

The simulation results are presented in the figures 3 and 4. Fig. 3 shows the plot of the x component of velocity $\langle V_x(y, t_n) \rangle_{x,n}$, measured at the times $t_n = nT$, $n = 1, \dots$ and averaged over x and n . In the Fig.4 the square root of mean square velocity $\sqrt{\langle V_x^2(y, t) \rangle_{x,t}}$ is plotted as a function of distance from the wall y . We observe that $\Re(k) \approx 0.63$ (wavelength of oscillation is equal to 10) and $\Im(k) \approx 0.21$, which, given the discrete nature of the LB simulations, is in good agreement with the theoretical values (15). For illustrative purposes, Figs. 3,4 contain results obtained using similar system, but without the elastic effects ($\mu = 0$), for which $\Im(k)/\Re(k) = 1$.

Finally, let us consider one more example on which the viscoelastic properties of our LB approach can be quantitatively studied: a periodically volume-driven fluid in a capillary. The model consists of a 9×128 elongated lattice with stick boundary conditions for long walls and periodic boundary conditions for short walls. A uniform time-periodic volume force $F_y = F_0 \cos(\omega t)$, directed along the longer walls, is applied to the fluid in the capillary. In the LB update scheme (6) it is implemented by adding the driving force $F_y(t)$ to the elastic force \vec{F}_{el} in the relaxation term on the right hand side of the lattice equation.

As the fluid in the capillary exhibits shear elasticity, there should be a resonance when the driving frequency ω coincides with the intrinsic oscillation frequency Ω of elastic media in the capillary. To study the resonance, we look at the driven oscillations of the first Fourier harmonic of velocity along the applied force,

$$\tilde{V}_{1y}(t) = \frac{2}{L_x L_y} \int_0^{L_x} \int_0^{L_y} \sin\left(\frac{x}{L_x} \pi\right) V_y(x, y, t) dx dy, \quad (16)$$

where the integration on dy stands for averaging along the length of the capillary. In the presence of volume force $F_y(t)$, a linearized Navier-Stokes equation yields for

the steady state amplitude of the first Fourier harmonic \tilde{V}_{1y} :

$$\tilde{V}_{1y} = \frac{4F_0}{qL_x} \frac{1}{q^2[\nu + \frac{\mu}{1+\omega^2\tau^2}] + i\omega[\frac{q^2\mu\tau}{1+\omega^2\tau^2} - 1]}, \quad (17)$$

where $q = \pi/L_x$ is a wavevector of the first harmonic. The resonance is achieved when the absolute value of this expression has the maximum, i.e. when the second bracket in denominator becomes equal to zero,

$$\omega = \Omega \equiv \frac{1}{\tau} \sqrt{q^2\mu\tau - 1} \quad (18)$$

Also, when a system is in resonance, there no phase shift between driving force and induced oscillation so that the ratio between the force and the oscillation amplitudes is real. To check whether our LB model behaves as predicted by the continuous Navier-Stokes equation, we performed a simulation using the following parameters: $\mu = 0.3$, $\lambda = -1.5$, $\tau = 250$, $F_0 = 0.001$; frequency of the drive ω was equal to $\Omega \approx 0.011$, $\Omega/2$, and 2Ω . The measured values of the \tilde{V}_{1y} are presented in Fig.5.

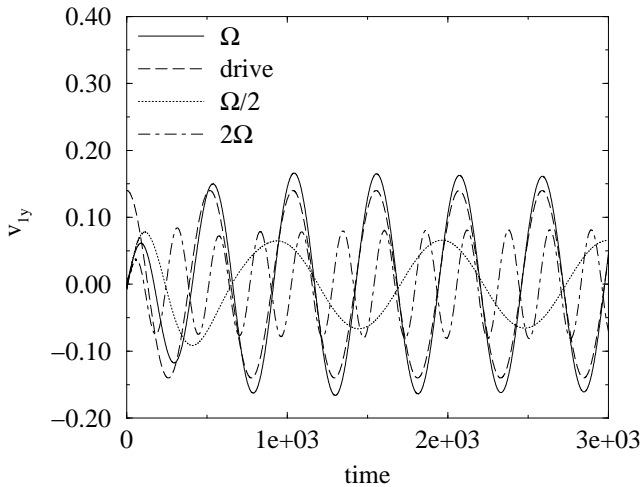


Fig. 5. Amplitude of the first Fourier harmonic \tilde{V}_{1y} as a function of time for different driving frequencies, $\omega = \Omega$, $\omega = 2\Omega$, $\omega = \Omega/2$.

After a short transient period the system approaches the steady state. As predicted by (17), for resonant drive ($\omega = \Omega$) the steady state amplitude of oscillation $\tilde{V}_{1y} \approx 0.16$; while for off-resonance drive, $\omega = \Omega/2$ and $\omega = 2\Omega$, the amplitudes \tilde{V}_{1y} are at least twice smaller. To study a phase shift between the drive and induced oscillations, we also plotted a driving force for the resonant

frequency, $F(t) \sim \cos(\Omega t)$. One can observe that there is no visible phase shift between driving and induced oscillation, which confirms that the shear elastic resonance frequency of our LB model is well reproduced by the continuous expression (18). We also observe that when the drive frequency ω is below or above the resonance frequency Ω , the induced oscillations are phase-delayed and phase-advanced, respectively, which again follows from (18).

Three examples, considered in this section, indicate that for a variety of physical systems, the behavior of the proposed viscoelastic LB model is qualitatively and quantitatively described by the continuous Navier-Stokes equations with Maxwell viscoelastic term. It allows us to conclude that our model indeed reproduces the Maxwell viscoelasticity for the incompressible fluid flow.

III. CONCLUSION

We proposed a simple yet versatile approach of incorporating viscoelastic effects into Lattice Boltzmann simulations for 6-velocity 2D BGK model Generalization for more sophisticated LB schemes which includes 3D and higher-velocity models is straightforward. Although, for computational stability and efficiency reasons, our approach has not yet allowed us to reach a limit of pure elastic solids, it works well in the range of parameters typical for most naturally-occurring viscoelastic media. We leave consideration of more sophisticated than the Maxwell viscoelastic models for the future.

-
- [1] G. R. McNamara and G. Zanetti, Phys. Rev. Lett. **61**, 2332 (1988).
 - [2] F. J. Higuera and J. Jimenes, Europhys. Lett. **9**, 663 (1989).
 - [3] H. D. Chen, S. Y. Chen, and W. Mattheus, Phys. Rev. A **45**, R5339 (1992).
 - [4] S. Chen and G. D. Doolen, Annu. Rev. Fluid Mech. **30**, 329 (1998).
 - [5] Y. H. Qian and Y. F. Deng Phys. Rev. Lett. **79**, 2742 (1997).
 - [6] M. J. Crochet, A. R. Davies, and K. Walter, *Numerical Simulation of Non-Newtonian Flow*, Elsevier Science Publishers, Amsterdam, 1984.